

Toxic effects of ZnO NPs on immune response and tissue pathology in *Mytilus galloprovincialis*

Zihan Xing^{a,1}, Zimin Cai^{a,1}, Liuya Mi^{a,1}, Juan Zhang^b, Jiaying Wang^b, Lizhu Chen^b, Mingzhe Xu^a, Bangguo Ma^a, Ruijia Tao^a, Bowen Yang^c, Xinmeng Lv^a, Lei Wang^a, Yancui Zhao^a, Xiaoli Liu^{a,*}, Liping You^{b,*}

^a School of Life Sciences, Ludong University, Yantai, 264025, PR China

^b Shandong Key Laboratory of Marine Ecological Restoration, Shandong Marine Resources and Environment Research Institute, Yantai, 264006, PR China

^c Department of Chemistry, University of Alberta, Edmonton, Alberta, T6G 2G2, Canada

ARTICLE INFO

Keywords:

ZnO NPs

Mytilus galloprovincialis

Toxicity

Gene expression

Tissue pathology

ABSTRACT

Nano-zinc oxide (ZnO NPs), as widely used nanomaterials, are inevitably released into aquatic environments, posing potential threats to aquatic organisms. *Mytilus galloprovincialis* is a bivalve species sensitive to changes in marine ecological environments, but there has been limited research on its toxicity response to ZnO NPs. Therefore, we selected *M. galloprovincialis* as the research subject and exposed them to 50 µg/L ZnO NPs for 96 h and 30 days to determine the dissolution of ZnO NPs in seawater and their distribution in *M. galloprovincialis*. The toxicity of ZnO NPs in *M. galloprovincialis* was then evaluated through gene expression, tissue pathology, and cellular immune response. The results showed that ZnO NPs could enrich Zn in various tissues of the mussel, in the order of gills > hepatopancreas > adductor muscle > mantle. Seven immune-related genes including four heat shock protein genes (*HSPA12A*, *sHSP24.1*, *sHSP22*, *TCTP*) and three apoptotic genes (*Ras*, *p63* and *Bcl-2*) were altered to varying degrees. There was a downward trend in lysosomal membrane stability of *M. galloprovincialis* after exposure to ZnO NPs for 96 h and 30 days, while ROS and apoptosis rates increased significantly. Furthermore, the seven genes, apoptosis, LMS, and ROS were dependent on exposure time, treatment, and their interaction. Histopathological damage included disorganisation of hepatopancreas epithelial cells, gill filament swelling, and contraction of blood sinuses. These results indicated that ZnO NPs exerted toxicity in *M. galloprovincialis*, affecting the immune system, resulting in changes in the expression of immune-related genes and ultimately leading to histopathological changes. Our research findings could contribute to systematically understand the impact of ZnO NPs on bivalves in aquatic environments and provide a theoretical basis for marine pollution assessment.

1. Introduction

ZnO NPs are widely used nanomaterials, with applications in photocatalysis, biomedical fields, the textile industry, and environmental protection (Al-Etaibi and El-Apasery, 2024; Asha et al., 2022; Matei et al., 2023; Sahebjam et al., 2024; Subramani and Incharoensakdi, 2024; Zhang et al., 2024). It is estimated that global production of ZnO NPs ranges from 550 to 33,400 tonnes per year, making it the third most widely produced metal nanoparticle globally (Fatima et al., 2024; Piccinno et al., 2012). However, the extensive use of ZnO NPs can lead to their accumulation in water bodies. The environmental sensitivity

sequence of aquatic organisms to ZnO NPs is as follows: invertebrates > bacteria > algae > vertebrates (Bordin et al., 2024). Bivalves, as typical representatives of invertebrates, are widely distributed in freshwater, estuarine, and marine ecosystems, which are the main gathering areas for environmental pollutants such as nanomaterials. Therefore, bivalves exhibit sensitive responses to the environmental changes and are considered good indicator organisms for environmental pollution (Weng et al., 2022).

ZnO NPs can enhance the activity of *Xenostrobus securis* GST and SOD, thereby causing oxidative stress (Lai et al., 2023). ZnO NPs induce oxidative damage to proteins and lipids in *Mytilus edulis*, as well as an

* Corresponding authors.

E-mail addresses: lxlshz2006@163.com (X. Liu), youliping521@163.com (L. You).

¹ Zihan Xing, Zimin Cai and Liuya Mi contributed equally to this work.

increase in the transcription levels of apoptosis-related genes (*p53*, *caspase 3*, *JNK* and *p38*), while the mRNA expression of the anti-apoptotic gene *Bcl-2* decreases (Wu et al., 2022). ZnO NPs lead to a significant decrease in total haemocyte count, phagocytic activity, esterase, and lysosomal content in *Mytilus coruscus*, while the haemocyte death rate and reactive oxygen species (ROS) increase (Wu et al., 2018). Overall, studies on the toxicity of ZnO NPs to bivalves have mainly focused on oxidative stress, genetic toxicity, and immune response. *M. galloprovincialis*, distributed in temperate and subpolar marine and estuarine areas, is an important species for aquaculture and is commonly used for environmental monitoring and toxicological assessment (Andrade et al., 2024; Ouagajjou et al., 2023). Research has found that ZnO NPs can induce respiratory bursts in *M. galloprovincialis* and lead to a decrease in lysosomal membrane stability in haemocytes (Ciacci et al., 2012; Efthimiou et al., 2021). Additionally, ZnO NPs can cause membrane damage and neurotoxicity in *M. galloprovincialis*, along with changes in enzyme activities (SOD, CAT, GPx) in gills and hepatopancreas (Bouzidi et al., 2024; Ciacci et al., 2012). Investigating the response characteristics of *M. galloprovincialis* to ZnO NPs can effectively reflect the impact of ZnO NPs on marine organisms.

In the present study, polyvinylpyrrolidone (PVP)-coated ZnO NPs were synthesised using the phosphate solution reduction method. Afterwards, the NPs were characterized via transmission electron microscopy (TEM), scanning electron microscopy (SEM), energy dispersive X-ray spectroscopy and dynamic light scattering (DLS). Subsequently, we conducted exposure experiments with ZnO NPs (50 µg/L) in *M. galloprovincialis*, and after 96 h and 30 days of exposure, we detected the dissolution of ZnO NPs in seawater and their accumulation characteristics in *M. galloprovincialis*. Through detection of tissue pathology, analysis of four heat shock protein genes (*heat shock 70 kDa protein 12A (HSPA12A)*, *small heat shock protein 24.1 (sHSP24.1)*, *small heat shock protein 22 (sHSP22)*, *translationally controlled tumor protein (TCTP)*) and three apoptotic genes (*ras proto-oncogene (Ras)*, *tumor protein p63 (p63)* and *B-cell lymphoma-2 (Bcl-2)*), apoptosis, lysosomal membrane stability (LMS) and ROS, we systematically studied the toxic effects of ZnO NPs in *M. galloprovincialis*. The results of this study could further enrich the existing literature regarding nanomaterials toxicity against bivalves in addition to contributing to the theoretical background with respect to the environmental risk assessment.

2. Materials and methods

2.1. Preparation and characterization of ZnO NPs

In this experiment, PVP-coated ZnO NPs were prepared using the phosphate solution reduction method, with the reaction equations as follows: $ZnCl_2 + 2H_3PO_2 + H_2O \rightarrow Zn + 2HPO_3 + 2HCl$, $Zn + H_2O \rightarrow ZnO + H_2$. First, the Zn oxide solution was prepared by mixing ZnCl₂ and deionised water, while the reducing solution was prepared by mixing H₃PO₂, PVP, Sodium hexametaphosphate (SHMP), and NaOH. Then, the Zn oxide solution and the reducing solution were preheated in a water bath at 42 °C. The Zn oxide solution was added dropwise into the reducing solution at a rate of 20 µL/5 s/drop while stirring continuously. After the addition was complete, stirring continued for 30 min. The mixture was then poured into tubes and allowed to stand for 1 h. Subsequently, the mixture was centrifuged at 10 °C and 9000 g for 30 min to remove the supernatant. The precipitate was then resuspended in a substrate using a passivating agent and subjected to ultrasonication for 20 min to ensure complete and uniform resuspension of the substrate. This centrifugation and resuspension process was repeated at 10 °C and 9000 g for 30 min to remove the supernatant. The precipitate was then resuspended in acetone and subjected to ultrasonication for approximately 20 min. The above centrifugation, resuspension in ethanol, and ultrasonication steps were repeated once more to ensure thorough purification of the substrate. Finally, the substrate was placed in a vacuum drying oven (Shenzhen Aodema Electronic Technology Co., Ltd, ZKGL-

6053) and dried overnight at 40–50 °C to collect ZnO NPs powder.

The morphology, particle size, and quality of ZnO NPs powder were analysed using

SEM (SEM-EDX, Hitachi, S-4800) and TEM (TEM, Hitachi, H-700). For SEM, ZnO NPs powder was dissolved in ethanol and ultrasonicated for 15 min, then evenly coated onto SEM sample holders with conductive carbon double-sided tape. The ZnO NP suspension was evenly applied to the surface of the conductive carbon double-sided tape. Detection was performed at an acceleration voltage of 5 kV and a magnification of 100 k. For TEM, 10 µL of ZnO NPs suspension was placed onto a grid for 1 min, then absorbed by filter paper and allowed to dry at room temperature for a few minutes before detection at 200 kV.

The diameter and zeta potential of ZnO NPs were analysed using Dynamic light scattering (DLS) technique (Malvern NanoZS, Malvern instruments limited). ZnO NPs were ultrasonicated in double-distilled water for 15 min to prepare a suspension. 1 mL of ZnO NPs suspension was added to the sample tube, ensuring complete coverage of the detection area, and measured three times for repeatability. The instrument was calibrated using polystyrene microspheres with a diameter of 200 nm and a concentration of 2.01×10^{10} particles/mL, and four different sizes (68 nm, 91 nm, 113 nm, and 155 nm) of uniformly dispersed silica microspheres were used as reference standards. The NanoFCM software NF Professional v1.08 was used to calculate particle concentration and size distribution, and R software v4.1.0 was used to calculate the median and interquartile range.

2.2. ZnO NPs exposure experiment

M. galloprovincialis was purchased from the Xin Hongli market in Yantai, China. The *M. galloprovincialis* had an average size of body length (6.12 ± 0.63) cm × body width (2.52 ± 0.34) cm × body thickness (1.52 ± 0.18) cm. They were acclimated for 10 days in plastic tanks (55 × 35 × 12 cm). There were 20 mussels in each tank, with 3 replicate tanks per group. Each plastic tank was filled with 5 L of seawater, with an average salinity of (31.2 ± 0.28) %, a temperature of (16.2 ± 0.28) °C, and a pH of 7.98 ± 0.04 . Continuous aeration was maintained using an air pump and airstones to ensure water circulation. The seawater was changed every 24 h, and 500 µL of concentrated *Chlorella vulgaris* microalgae was fed to each tank every 3 h before changing the seawater.

M. galloprovincialis was divided into a control group (0 µg/L ZnO NPs) and an experimental group (50 µg/L ZnO NPs), with each group containing 6 replicates. The concentration was based on the levels of ZnO NPs in seawater (Lai et al., 2023; Wu and Sokolova, 2021; Xu et al., 2023). At 96 h and 30 days of exposure, the hepatopancreas and gills were collected from *M. galloprovincialis*, washed with PBS buffer, and then fixed in paraformaldehyde for subsequent histopathological tissue section experiments. Hemocytes, hepatopancreas, gills, mantle, and adductor muscles were also collected, placed in 1.5 mL centrifuge tubes, quickly frozen in liquid nitrogen, and stored in an –80 °C ultra-low temperature freezer for subsequent toxicological effect experiments. Additionally, about 500 µL haemolymph were collected from the adductor muscles, centrifuged at 4 °C and 1774 g for 10 min, and resuspended in physiological saline for immune response experiments.

2.3. Detection of Zn content in seawater and *M. galloprovincialis*

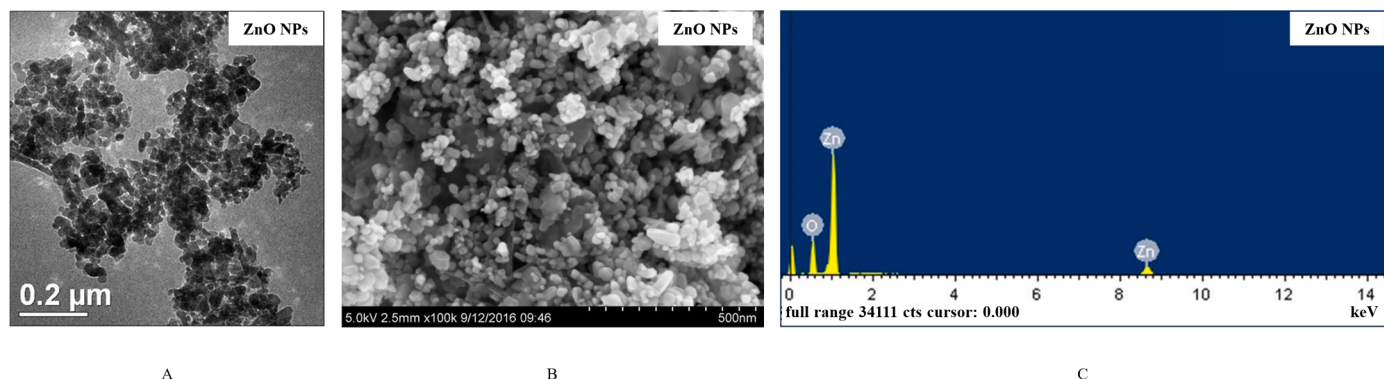
500 mL filtered seawater was taken and acidified with 5 mL of nitric acid. Then, 10 mL of concentrated nitric acid was added, heated, and evaporated to 20 mL. Next, 5 mL of concentrated nitric acid was added and heated until dry. Afterwards, 5 mL of concentrated hydrochloric acid was added, slightly heated, and mixed with 5 mL of sodium hydroxide solution (5 M concentration). The solution was then filtered, and the filtrate was added to 100 mL of deionised water. Zinc quantification was performed using ICP-MS (Agilent 7500i, Agilent Technologies Co. Ltd, USA).

The collected hepatopancreas, gills, mantle, and adductor muscles of

Table 1

The genes of primers used in the experiment of qRT-PCR.

Gene name	NCBI Accession number	Primers
heat shock 70 kDa protein 12A (<i>HSPA12A</i>)	JN232381.1	Forward (5'-3') Reverse (5'-3')
translationally controlled tumor protein (<i>TCTP</i>)	JN232382.1	Forward (5'-3') Reverse (5'-3')
small heat shock protein 22 (<i>sHSP22</i>)	JF803804.1	Forward (5'-3') Reverse (5'-3')
small heat shock protein 24.1 (<i>sHSPs24.1</i>)	JF803805.1	Forward (5'-3') Reverse (5'-3')
ras proto-oncogene (<i>Ras</i>)	DQ305041.1	Forward (5'-3') Reverse (5'-3')
tumor protein p63 (<i>P63</i>)	UYJE01000634.1	Forward (5'-3') Reverse (5'-3')
B-cell lymphoma-2 (<i>Bcl-2</i>)	UYJE01008498.1	Forward (5'-3') Reverse (5'-3')
28 s ribosomal RNA (28 s rRNA)	AB103129.1	Forward (5'-3') Reverse (5'-3')

**Fig. 1.** Characterization of ZnO NPs. A: The transmission electron microscope images of ZnO NPs; B: The scanning electron microscope images of ZnO NPs; C: The energy spectrum analysis diagrams of ZnO NPs.**Table 2**

The contents of Zn in seawater during the ZnO NPs experiment (μg/L).

Group	Time	Control	ZnO NPs
0 h		0.755	1.794
24 h		0.752	1.564
Ingestion rate (%)		–	12.8%

M. galloprovincialis were washed with pure water, dried at 80 °C to constant weight (10 – 20 mg per sample), accurately weighed, and placed in 1 mL of concentrated nitric acid (70 %, Fisher Scientific) for digestion using a microwave digestion instrument (CEM, MAR5). The heating program for samples in the microwave digestion instrument was set to 15 min of heating at 200 °C, followed by maintaining at 200 °C for 15 min. Each completely digested sample was diluted to 5 mL with ultrapure water, and Zn quantification was performed using ICP-MS (Agilent 7500 i, Agilent Technologies Co. Ltd, USA).

2.4. Expression changes of immune-related genes in *M. galloprovincialis*

The changes in transcription levels of four heat shock protein genes

(*HSPA12A*, *TCTP*, *sHSP22*, and *sHSP24.1*) and three apoptosis genes (*P63*, *Bcl-2*, and *Ras*) were detected using a 7500 real-time fluorescence quantitative PCR instrument (7500 Fast, Applied Biosystems). The PCR reaction conditions were: 50 °C for 2 min (1 cycle); 95 °C for 30 s (1 cycle); 95 °C for 5 s, 60 °C for 30 s (40 cycles). The housekeeping gene was 28 s rRNA and calculations were performed using the 2^{-ΔΔCt} method (Caykara et al., 2021; Cellura et al., 2006). The specific primer sequences are listed in Table 1.

2.5. Histopathological changes in *M. galloprovincialis*

The gills and hepatopancreas of *M. galloprovincialis* were fixed in paraformaldehyde at 4 °C for 12 h. Dehydration was then performed by sequentially immersing the samples in a gradient of 50%, 70%, 80%, 95%, and 100% ethanol to remove water. Then, samples were subsequently immersed in a 1:1 mixture of absolute ethanol and xylene, treated with xylene for transparency, and embedded in paraffin. The samples were sliced into 5 μm thick sections using a microtome (Leica RM2015, Leica Biosystems, Germany) and floated in a 40 °C water bath. The tissue sections were mounted on adhesive slides, deparaffinised with xylene, and rehydrated using a gradient of 100%, 95%, 85%, and

Table 3The tissue distributions of zinc in *Mytilus galloprovincialis* (μg/g dry weight).

Tissue	Hepatopancreas		Gills		Mantle		Muscle	
	Time	Group	96 h	30 d	96 h	30 d	96 h	30 d
Control	89.36±7.91		71.26±12.0	188.50±20.4	136.15±10.7	21.94±0.587	25.36±5.84	78.12±15.63
ZnO NPs	112.10±28.4		172.58±44.3	240.12±39.4	375.03±32.6	22.15±0.641	21.28±3.40	71.98±11.07

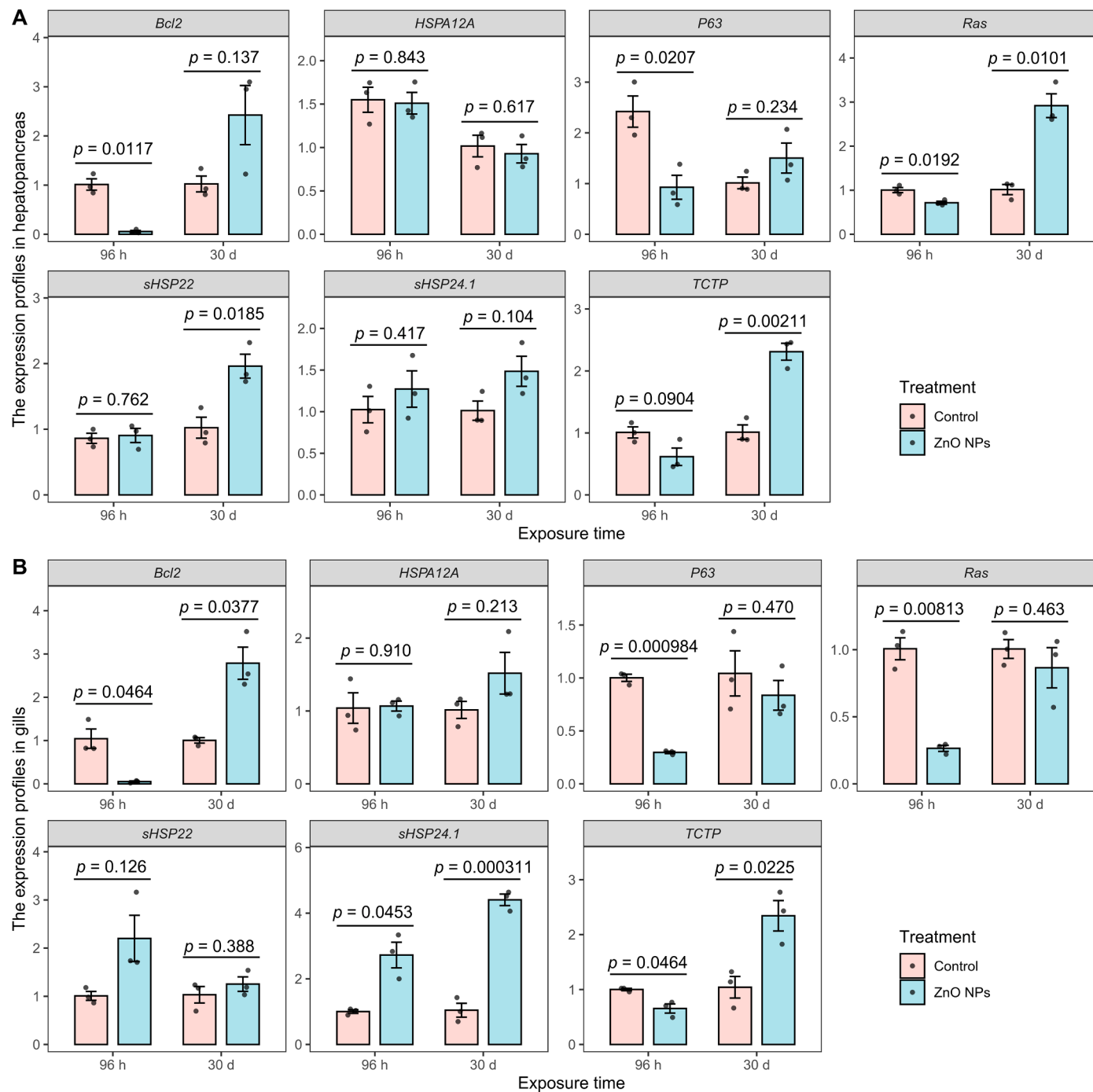


Fig. 2. Differences in the expression of seven genes between treatments with control and ZnO NPs in hepatopancreas and gills of *M. galloprovincialis* (Y-axis represented the relative quantitative expressions of the genes, and calculations were performed using the $2^{-\Delta\Delta Ct}$ method).

75% ethanol, and distilled water. They were then, stained with haematoxylin and eosin, dehydrated with 75%, 85%, 95%, and 100% ethanol, treated with xylene for transparency, and sealed with neutral gum. Tissue sections were observed under a microscope at 400x magnification and recorded.

2.6. The detection of apoptosis, LMS and ROS in hemolymph of *M. galloprovincialis*

500 μ L of hemolymph was mixed with 500 μ L of anticoagulant (glucose 20.8 g/L, sodium citrate 8.0 g/L, EDTA 3.36 g/L, sodium chloride 22.5 g/L, pH = 7.5) at a 1:1 ratio. After centrifugation at 300 g

for 10 min at 4 °C, the supernatant was removed, and the hemocytes were collected. The hemocytes were then resuspended in 1 mL of PBS (pH 7.4, 2% NaCl), centrifuged at 2000 g for 10 min at 4 °C, and the supernatant was discarded. A further, 1 mL of PBS was added to resuspend the hemocytes for subsequent testing.

Apoptosis in the hemolymph was measured using a double staining kit (Annexin V-FITC and PI). 500 μ L of the kit buffer was mixed with hemocytes, 5 μ L of Annexin V-FITC was added, and the mixture was incubated at room temperature (18–20 °C) in the dark for 5–10 min, followed by the addition of 5 μ L of PI and incubation at room temperature (18–20 °C) in the dark for an additional 5 min. Flow cytometry analysis was performed (Annexin V-FITC green fluorescence using the

Table 4

Effects of treatment (ZnO NPs vs. control), exposure time (96 h vs. 30 days), and their interaction on the expression of seven genes in the hepatopancreas and gills. The *p* values are from ANOVAs (*n* = 12).

Gene name	Response	Predict	DF	F value	<i>p</i> value
<i>Bcl2</i>	Expression in hepatopancreas	Time	1,8	14.1	0.00556
<i>Bcl2</i>	Expression in hepatopancreas	Treatment	1,8	0.5	0.504
<i>Bcl2</i>	Expression in hepatopancreas	Time × Treatment	1,8	13.9	0.00585
<i>Bcl2</i>	Expression in gills	Time	1,8	37.8	0.000275
<i>Bcl2</i>	Expression in gills	Treatment	1,8	3.2	0.109
<i>Bcl2</i>	Expression in gills	Time × Treatment	1,8	40	0.000227
<i>HSPA12A</i>	Expression in hepatopancreas	Time	1,8	19.7	0.00216
<i>HSPA12A</i>	Expression in hepatopancreas	Treatment	1,8	0.3	0.621
<i>HSPA12A</i>	Expression in hepatopancreas	Time × Treatment	1,8	0	0.851
<i>HSPA12A</i>	Expression in gills	Time	1,8	1.3	0.293
<i>HSPA12A</i>	Expression in gills	Treatment	1,8	2	0.198
<i>HSPA12A</i>	Expression in gills	Time × Treatment	1,8	1.6	0.244
<i>P63</i>	Expression in hepatopancreas	Time	1,8	2.7	0.136
<i>P63</i>	Expression in hepatopancreas	Treatment	1,8	4	0.0808
<i>P63</i>	Expression in hepatopancreas	Time × Treatment	1,8	15.6	0.00422
<i>P63</i>	Expression in gills	Time	1,8	5.1	0.054
<i>P63</i>	Expression in gills	Treatment	1,8	12.5	0.00764
<i>P63</i>	Expression in gills	Time × Treatment	1,8	3.7	0.0894
<i>Ras</i>	Expression in hepatopancreas	Time	1,8	53.9	8.07 × 10 ⁻⁵
<i>Ras</i>	Expression in hepatopancreas	Treatment	1,8	28.7	0.000681
<i>Ras</i>	Expression in hepatopancreas	Time × Treatment	1,8	52.8	8.68 × 10 ⁻⁵
<i>Ras</i>	Expression in gills	Time	1,8	10.4	0.0123
<i>Ras</i>	Expression in gills	Treatment	1,8	22.5	0.00146
<i>Ras</i>	Expression in gills	Time × Treatment	1,8	10.5	0.0119
<i>sHSP22</i>	Expression in hepatopancreas	Time	1,8	19.5	0.00224
<i>sHSP22</i>	Expression in hepatopancreas	Treatment	1,8	12.6	0.00746
<i>sHSP22</i>	Expression in hepatopancreas	Time × Treatment	1,8	10.5	0.0119
<i>sHSP22</i>	Expression in gills	Time	1,8	2.9	0.125
<i>sHSP22</i>	Expression in gills	Treatment	1,8	6.9	0.0306
<i>sHSP22</i>	Expression in gills	Time × Treatment	1,8	3.2	0.109
<i>sHSP24.1</i>	Expression in hepatopancreas	Time	1,8	0.3	0.577
<i>sHSP24.1</i>	Expression in hepatopancreas	Treatment	1,8	4.3	0.0705
<i>sHSP24.1</i>	Expression in hepatopancreas	Time × Treatment	1,8	0.4	0.532
<i>sHSP24.1</i>	Expression in gills	Time	1,8	12.9	0.00711
<i>sHSP24.1</i>	Expression in gills	Treatment	1,8	112	5.55 × 10 ⁻⁶
<i>sHSP24.1</i>	Expression in gills	Time × Treatment	1,8	11.7	0.00908
<i>TCTP</i>	Expression in hepatopancreas	Time	1,8	48.1	0.00012
<i>TCTP</i>	Expression in hepatopancreas	Treatment	1,8	13.7	0.00609
<i>TCTP</i>	Expression in hepatopancreas	Time × Treatment	1,8	47.6	0.000125
<i>TCTP</i>	Expression in gills	Time	1,8	24.4	0.00114
<i>TCTP</i>	Expression in gills	Treatment	1,8	7.4	0.026
<i>TCTP</i>	Expression in gills	Time × Treatment	1,8	22.1	0.00154

FL-1 channel, PI red fluorescence using the FL-2 channel), and the results were expressed as the percentages of FITC-positive and PI-positive cells relative to the total number of cells.

The LMS was measured using the neutral red spectrophotometric method. 500 μL of the working solution was added to 50 μL of PBS (containing 0.33% neutral red, 2% NaCl), incubated at 10 °C for 1 h, and then centrifuged at 300 g for 10 min. After centrifugation, the supernatant was discarded, and the cells were washed twice with PBS. Next, 500 μL of ice-cold acetic acid (1%, prepared in 50% alcohol solution) was added and incubated at 20 °C in the dark for 15 min. The samples were measured on a spectrophotometer (Infinite M200, Switzerland,) at 550 nm excitation wavelength, and the results were expressed as OD₅₅₀/mg hemocyte protein.

ROS was assessed by measuring the respiratory burst production. 500 μL of the working solution was added to 1.5 mL Eppendorf tubes, and 5 μL of the fluorescent probe DCFH-DA (2', 7'-Dichlorofluorescent yellow diacetate DCFH-DA) was added to achieve final concentration of 0.01 mmol/L. The tubes were incubated at 18 °C in the dark for 1 h. The fluorescence intensity of DCF was detected using a flow cytometer with an excitation wavelength of 488 nm and an emission wavelength of 525 nm. The production of ROS was expressed as the fluorescence intensity of DCF.

2.7. Statistical analysis

Data were presented as Mean ± Standard error. To assess the differences in gene expression, apoptosis, LMS, and respiratory burst between ZnO NPs treatment and control at each exposure time, two-sided *t*-tests in R (version 4.3.1) were performed in both the hepatopancreas and gills of *M. galloprovincialis*. To investigate the effects of exposure time and ZnO NPs treatment on gene expression, LMS, respiratory burst, and apoptosis, ANOVA using the *anova()* R function was performed and tested whether the every index in the hepatopancreas and gills depended on exposure time, ZnO NPs treatment, and their interaction. Correlation coefficients for the expression of genes, LMS, respiratory burst, and apoptosis in the hepatopancreas and gills were calculated using the *cor()* R function. Principal Component Analysis (PCA) was performed to reduce the dimensionality of the data and identify patterns or clusters among samples. The analyses were conducted across the conditions of ZnO NPs treatment and exposure time using the *prcomp()* R function for both hepatopancreas and gills. The *manova()* R function was used to test whether PC1 and PC2 depended on these conditions.

3. Results

3.1. Characterization of ZnO NPs

The characterization of ZnO NPs was examined by TEM and SEM. Fig. 1A shows the TEM images of ZnO NPs, which exhibit a uniform shape distribution with a small variation in particle size, averaging 20 nm. Fig. 1B shows the SEM images of ZnO NPs, indicating spherical particles uniformly dispersed in the solution without aggregation. Energy-dispersive X-ray spectroscopy analysis confirmed the presence of Zn and O in ZnO NPs, as shown in Fig. 1C. DLS analysis of the nano-powder suspension yielded a diameter of approximately 363.3 nm. The zeta potential test results showed absolute values were greater than 30 mV. Usually the system is stable when the absolute value of zeta potential is greater than 30 mv. In a word, it can be seen from Fig. 1 that the properties of PVP coated ZnO NPs were stable, which layed a good foundation for subsequent experiments.

3.2. Zn content in seawater and *M. galloprovincialis*

Table 2 indicates changes in Zn content in seawater after 24 h of exposure to ZnO NPs, with a decrease observed in the ZnO NPs group, showing a consumption rate of 12.8%. The distribution of Zn in

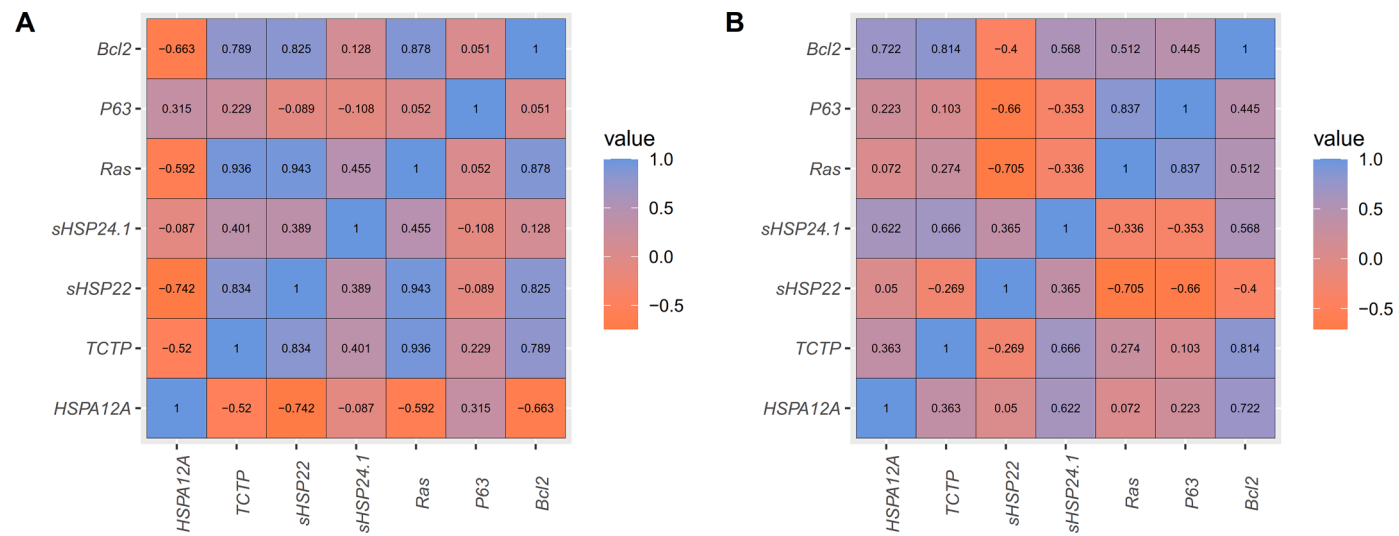


Fig. 3. Correlation coefficients of the expression of seven genes in hepatopancreas and gills of *M. galloprovincialis*. (A: hepatopancreas. B: gills)

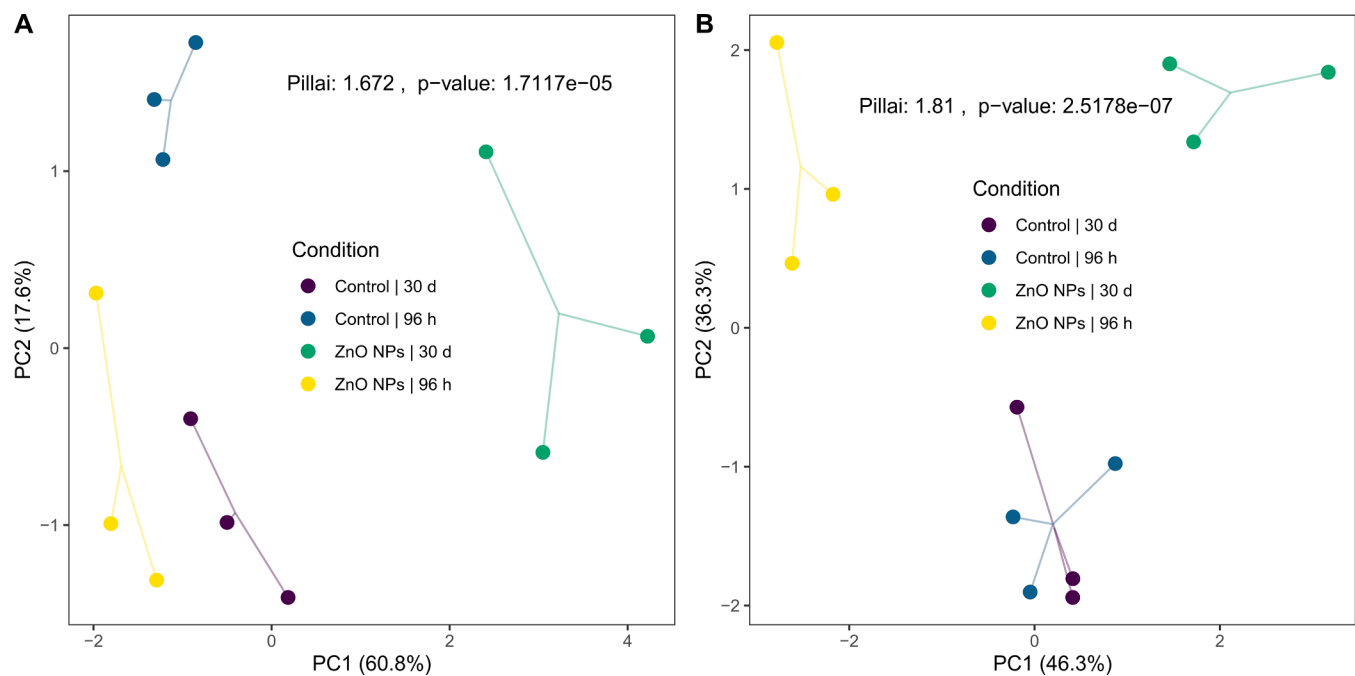


Fig. 4. Principal Component Analysis of gene expression levels in hepatopancreas and gills of *M. galloprovincialis* for the treatment conditions (ZnO NPs vs. control) and exposure time (96 h vs. 30 d). (A: hepatopancreas. B: gills)

M. galloprovincialis is shown in Table 3, with the order of Zn enrichment in tissues as follows: gills > hepatopancreas > adductor muscles > mantle.

3.3. Expression changes of seven genes in *M. galloprovincialis*

Differences in the expression of seven genes between treatments with ZnO NPs and control in hepatopancreas and gills of *M. galloprovincialis* are shown in Fig. 2. In the hepatopancreas of *M. galloprovincialis*, the expression of *Bcl-2* significantly increased, while *p63* decreased at 96 h, *sHSP22* and *TCTP* significantly increased at 30 days, and *Ras* significantly decreased at 96 h but increased at 30 d; In the gills of *M. galloprovincialis*, the expression of *p63* and *Ras* significantly decreased, while *Bcl-2* decreased at 96 h but increased at 30 days. Both *sHSP24.1* and *TCTP* significantly increased at 96 h and 30 days.

The effects of treatment (ZnO NPs vs. control), exposure time (96 h

vs. 30 days), and their interaction on the expression of seven genes in the hepatopancreas and gills are shown in Table 4. The *p* values are derived from ANOVAs (*n* = 12). As shown in the table, the expression of these seven genes was dependent on exposure time, treatment, and their interaction. Correlation coefficients of the expression of seven genes in hepatopancreas and gills are shown in Fig. 3, and Principal Component Analysis (PCA) of gene expression levels in hepatopancreas and gills for the treatment conditions (ZnO NPs vs. control) and exposure time (96 h vs. 30 days) are shown in Fig. 4. The first principal component (PC1) explained 60.8% of the total variance in gene expression in the hepatopancreas and 46.3 % in the gills, while the second principal component (PC2) accounted for 17.6% in the hepatopancreas and 36.3 % in the gills. Together, PC1 and PC2 explained 78.4% of the total variance in the hepatopancreas and 82.6% in the gills. Different treatment conditions and exposure times were separated, suggesting that these conditions had a pronounced effect on the gene expression profile in the

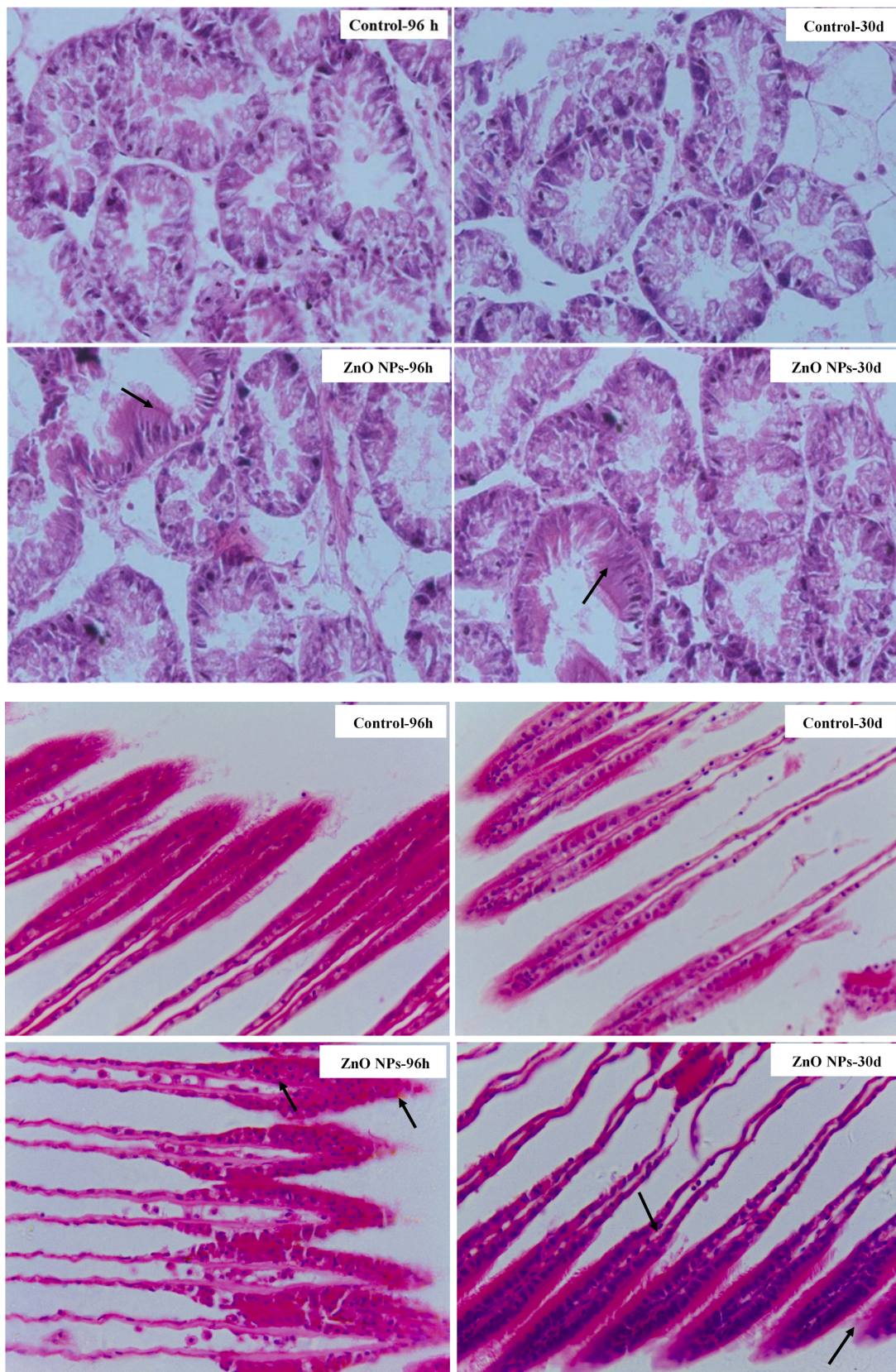


Fig. 5. A. The hepatopancreas histopathology images of *M. galloprovincialis* after exposure to ZnO NPs.
Fig. 5B. The gill histopathology images of *M. galloprovincialis* after exposure to ZnO NPs.

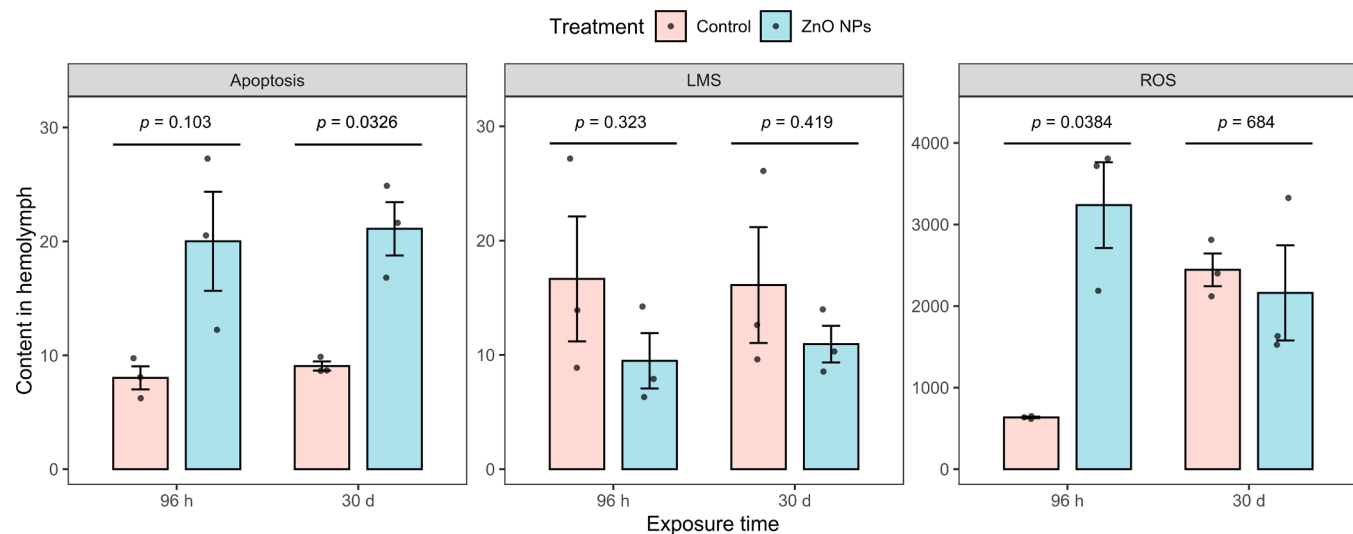


Fig. 6. The results of apoptosis, LMS, and ROS levels in the hemolymph of *M. galloprovincialis*. Y-axis of Apoptosis is Early apoptosis rate (%), LMS is Lysosomal membrane stability (OD₅₅₀/mg Protein), ROS is DCF fluorescence intensity.

Table 5

Effects of treatment (ZnO NPs vs. control), exposure time (96 h vs. 30 days), and their interaction on Apoptosis, LMS and ROS in the hepatopancreas and gills. The *p* values are from ANOVAs (*n* = 12).

Name	Response	Predict	DF	F value	p value
Apoptosis	Content in hemolymph	Time	1,8	0.2	0.684
Apoptosis	Content in hemolymph	Treatment	1,8	22.6	0.00144
Apoptosis	Content in hemolymph	Time × Treatment	1,8	<0.1	0.99
LMS	Content in hemolymph	Time	1,8	<0.1	0.912
LMS	Content in hemolymph	Treatment	1,8	2.4	0.162
LMS	Content in hemolymph	Time × Treatment	1,8	0.1	0.809
ROS	Content in hemolymph	Time	1,8	0.8	0.393
ROS	Content in hemolymph	Treatment	1,8	8.2	0.0211
ROS	Content in hemolymph	Time × Treatment	1,8	12.7	0.00739

hepatopancreas (MANOVA: Pillai = 1.672, *p* = 1.71 × 10⁻⁵) and gills (MANOVA: Pillai = 1.81, *p* = 2.52 × 10⁻⁵) of *M. galloprovincialis*.

3.4. Histopathological changes in *M. galloprovincialis*

The histopathological changes in the hepatopancreas and gills of *M. galloprovincialis* are illustrated in Fig. 5. In the control groups, the tissues exhibited normal structures without damage. In Fig. 5A, the arrangement of epithelial cells in the hepatopancreas was damaged in the ZnO NPs-treated group. Fig. 5B shows that the main pathological changes included swelling of the gill filaments and contraction of the blood sinuses.

3.5. Measurement of apoptosis, LMS, and ROS levels in *M. galloprovincialis*

The results of apoptosis, LMS, and ROS levels are shown in Fig. 6. Early apoptosis rates increased significantly after 30 days of exposure. After 96 h and 30 days of exposure to ZnO NPs in *M. galloprovincialis*, LMS showed varying degrees of decline, but this was not significant. The

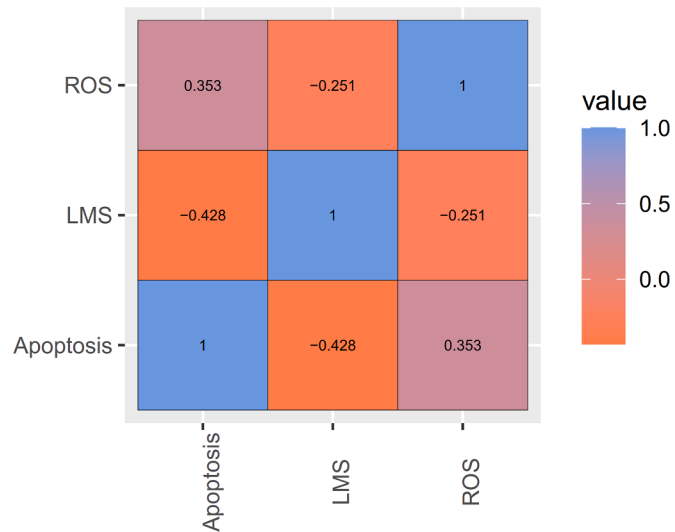


Fig. 7. Correlation coefficients for three indicators (apoptosis, LMS, and ROS) in the hemolymph of *M. galloprovincialis*.

production of ROS, expressed as the fluorescence intensity of DCF, significantly increased at 96 h, indicating a stress response; however, after 30 days, ROS levels decreased, although not significantly, suggesting an adaptation to prolonged exposure.

The effects of treatment (ZnO NPs vs. control), exposure time (96 h vs. 30 days), and their interaction on the expression of apoptosis, LMS, and ROS in the hemolymph are shown in Table 5. The *p*-values are derived from ANOVAs (*n* = 12). As shown in the table, these three indicators were dependent on exposure time, treatment, and their interaction. Correlation coefficients for these three indicators in the hemolymph are shown in Fig. 7, and Principal Component Analysis (PCA) for the treatment conditions (ZnO NPs vs. control) and exposure time (96 h vs. 30 days) is shown in Fig. 8. The figure shows that PC1 explained 56.4% of the total variance, while PC2 accounted for 25.2%. Together, PC1 and PC2 explained 81.6% of the total variance. Different treatment conditions and exposure times were separated, suggesting that these conditions had a pronounced effect on the apoptosis, LMS, and ROS profiles in the hepatopancreas (MANOVA: Pillai = 1.125, *p* = 0.02) of *M. galloprovincialis*.

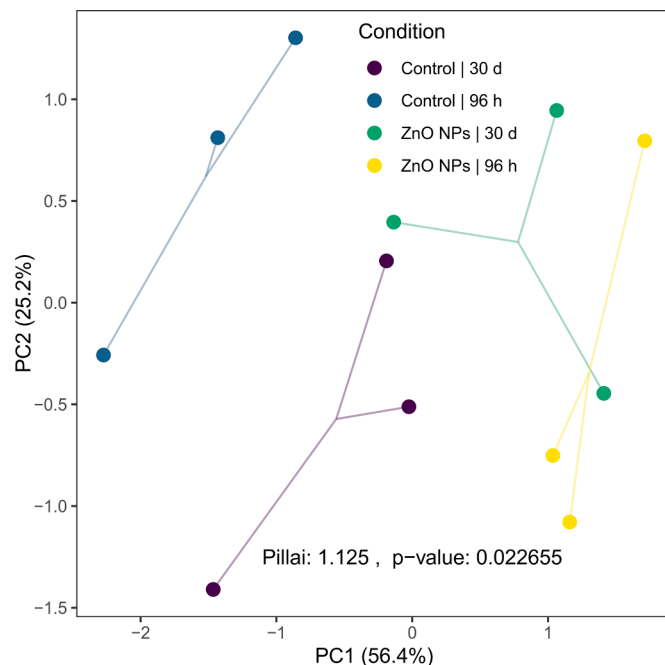


Fig. 8. Principal Component Analysis of apoptosis, LMS, and ROS in hemolymph of *M. galloprovincialis* for the treatment conditions (ZnO NPs vs. control) and exposure time (96 h vs. 30 days).

4. Discussion

ZnO NPs can be synthesised using physical and chemical methods (Matei et al., 2023). Ensuring uniform particle size, preventing aggregation between particles, and maintaining the stability of the suspension are key indicators of nanomaterials. The stability of nanomaterials can be enhanced by using capping and stabilising agents such as PVP. In this experiment, PVP-coated ZnO NPs met the expected particle size criteria, exhibited a uniform shape distribution with minimal variation in particle size, and thus met the required standards, laying a solid foundation for subsequent toxicological experiments.

Bivalves are widely used as bioindicators for monitoring marine environmental pollution (Sturla Lompré et al., 2024). The gills serve as the first point of entry for pollutants, which then move to the hepatopancreas through the mouth (Pizzurro et al., 2023). Therefore, both gills and hepatopancreas are crucial organs responsible for physiological processes such as respiration, feeding, and metabolism (Moreira et al., 2023; Wang et al., 2018). In our experiment, the gills and hepatopancreas showed the highest accumulation of Zn; thus, these two organs were selected for subsequent histopathological evaluations. Furthermore, structural abnormalities and functional impairments were observed in the gills and hepatopancreas of *M. galloprovincialis*, indicating that ZnO NPs could cause significant histopathological damage.

In our experiment, four heat shock protein genes (*HSPA12A*, *TCTP*, *sHSP22*, and *sHSP24.1*) changed to varying degrees. *HSPA12A* plays a crucial role in cellular responses to environmental stress, autophagy, protein folding, and degradation processes (Franzellitti et al., 2020). *TCTP* is involved in regulating cell proliferation, differentiation, and apoptosis (Bae et al., 2023). Both of these genes are implicated in protecting bivalves against environmental stressors such as zinc and cadmium challenges (Kim et al., 2024; You et al., 2013). In our experiment, *TCTP* was significantly elevated in both the hepatopancreas and gills, making it a potential biomarker for ZnO NPs stress. Although there were changes in *HSPA12A*, these were not statistically significant, rendering it less suitable for indicating ZnO NPs stress. *sHSP24.1* and *sHSP22* are members of the small heat shock protein family; they participate in cellular protective mechanisms by preventing protein aggregation and abnormal folding under stress conditions (Pei et al., 2024). The significant increase in *sHSP22* and *sHSP24.1* in *M. galloprovincialis* after exposure to ZnO NPs suggests that these two genes are good indicators of long-term exposure to materials.

The expression of three apoptosis-related genes (*P63*, *Bcl-2*, and *Ras*) also changed in *M. galloprovincialis* after exposure to ZnO NPs. *P63*, a member of the *p53* family, has been reported to have its DNA binding strongly inhibited by cadmium (Zylicz, 2001) (Adámik et al., 2015). *p63* also plays a crucial role in development and tissue repair (Ruiz et al., 2015). In our experiment, ZnO NPs caused histopathological changes in hepatopancreas and gills of *M. galloprovincialis*, leading to secondary changes in *p63*. Exposure to zinc sulfate has been shown to decrease *Bcl-2* expression (Ku et al., 2012), and we observed similar results with *p63* significantly decreasing after 96 h of exposure to ZnO NPs in the

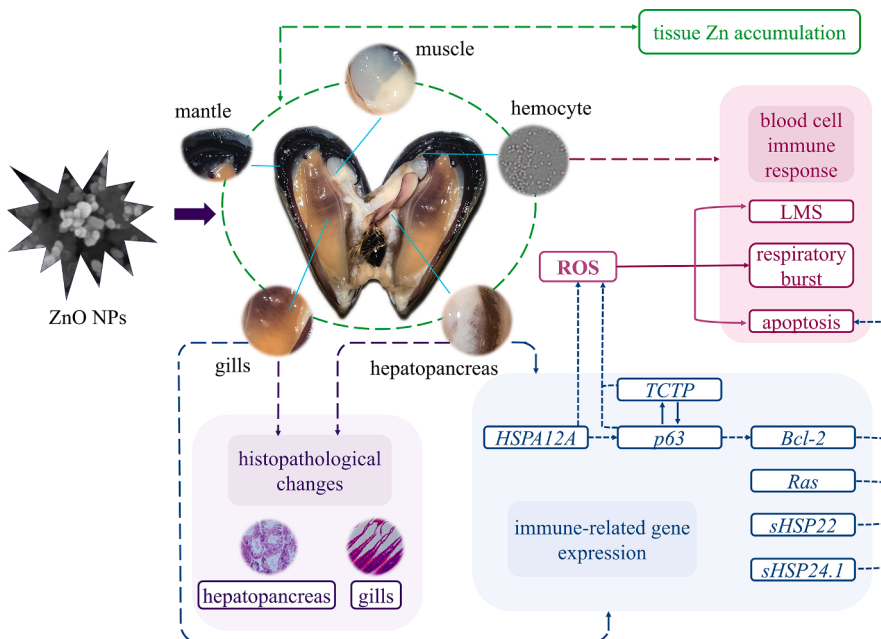


Fig. 9. The changes in *M. galloprovincialis* subjected to ZnO NPs stress.

gills. *Ras* is crucial for regulating cell growth, differentiation, and survival (Lima et al., 2008; Ruiz et al., 2015), and its elevation following nanomaterial stress could indicate a new marker.

Bivalves exhibit a highly sensitive response to pollutants, with the hemolymph serving as one of their primary defense mechanisms (Asnicar et al., 2024). Hemocytes recognize potential pathogens and particles through phagocytosis and cytotoxic reactions, releasing lysosomal enzymes into the hemolymph (Destoumieux-Garzón et al., 2020). Environmental stressors may lead to changes in membrane systems and lysosomal rupture, which are considered markers of cellular damage (Romdhani et al., 2022). In our experiment, ROS levels significantly increased in hemocytes after 96 h of exposure to ZnO NPs, indicating a stress response. Although ROS levels decreased after 30 days, the initial significant increase suggests a notable stress reaction to Zn nanoparticles. Early apoptosis rates also increased after 30 days of exposure, consistent with the observed respiratory burst response. Similar results have been reported in studies of the effects of ZnO NPs on the immune parameters of *Mytilus coruscus* hemocytes, indicating that ZnO NPs can indeed affect the immune system of bivalves, as well as their adaptability and survival in the external environment (Wu et al., 2018).

The changes in *M. galloprovincialis* subjected to ZnO NPs stress are illustrated in Fig. 9, depicting a process of mutual influence and causation. ZnO NPs were enriched in various tissues of *M. galloprovincialis* especially in the gills and hepatopancreas, leading to immune related responses and ultimately causing histopathological changes. The interaction between these factors requires further study in the future. Furthermore, the expression of seven genes, apoptosis, LMS, and ROS in the hepatopancreas and gills depended on exposure time, treatment, and their interaction.

5. Conclusion

In conclusion, our study revealed the following findings: First, ZnO NPs induced the accumulation of Zn in freshwater and various tissues of *M. galloprovincialis*. The order of Zn accumulation in *M. galloprovincialis* was as follows: gills > hepatopancreas > adductor muscle > mantle. Second, ZnO NPs impacted the expression of four heat shock protein genes and three apoptotic genes, accompanied by a significant decrease of LMS, increases of ROS and apoptosis during the exposure. Furthermore, the seven genes, apoptosis, LMS, and ROS were all dependent on exposure time, treatment, and their interaction. Third, ZnO NPs exposure caused histopathological changes in *M. galloprovincialis*, including disruption of the arrangement of epithelial cells in the hepatopancreas and morphological alterations. These results could underscore the multifaceted impact of ZnO NPs on bivalve molluscs. Overall, our research contributes to a systematic understanding of the impact of ZnO NPs on bivalves in aquatic environments and provides a theoretical basis for marine pollution assessment.

In our limited study, we didn't provide data on the aggregation state at the beginning and end of the ZnO NPs exposure periods, we will continue to explore this in future studies. Meanwhile, its deep mechanism to bivalves needs to be further explored.

Ethical approval

This article does not contain any studies with human participants or animals performed by any of the authors.

CRediT authorship contribution statement

Zihan Xing: Writing – original draft. **Zimin Cai:** Methodology. **Liuya Mi:** Methodology. **Juan Zhang:** Data curation. **Jiaying Wang:** Formal analysis. **Lizhu Chen:** Investigation. **Mingzhe Xu:** Methodology. **Bangguo Ma:** Software. **Ruijia Tao:** Methodology. **Bowen Yang:** Software. **Xinmeng Lv:** Data curation. **Lei Wang:** Investigation. **Yancui Zhao:** Methodology. **Xiaoli Liu:** Writing – review & editing,

Supervision. **Liping You:** Supervision.

Declaration of competing interest

The authors declare the following financial interests/personal relationships which may be considered as potential competing interests:

Xiaoli Liu reports financial support was provided by Ludong University. If there are other authors, they declare that they have no known competing financial interests or personal relationships that could have appeared to influence the work reported in this paper.

Data availability

Data will be made available on request.

Acknowledgements

This work was supported by the National Natural Science Foundation of China (grant number 32070126; 41506190), Talent Induction Program for Youth Innovation Teams in Colleges and Universities of Shandong Province (2022–2024).

References

- Adámik, M., Bažantová, P., Navrátilová, L., Polášková, A., Pečinka, P., Holáňová, L., Tichý, V., Brázdrová, M., 2015. Impact of cadmium, cobalt and nickel on sequence-specific DNA binding of p63 and p73 in vitro and in cells. *Biochem. Biophys. Res. Commun.* 456, 29–34. <https://doi.org/10.1016/j.bbrc.2014.11.027>.
- Al-Etaibi, A.M., El-Apaser, M.A., 2024. A Holistic Review of 3-Dimethylamino-1-Arylpropenones Based Disperse Dyes for Dyeing Polyester Fabrics: synthesis, Characterization, and Antimicrobial Activities. *Polymers. (Basel)* 16, 453. <https://doi.org/10.3390/polym16040453>.
- Andrade, M., Pinto, J., Soares, A.M.V.M., Solé, M., Pereira, E., Freitas, R., 2024. How predicted temperature and salinity changes will modulate the impacts induced by terbium in bivalves? *Chemosphere* 351, 141168. <https://doi.org/10.1016/j.chemosphere.2024.141168>.
- Asha, S., Bessy, T.C., Joe Sherin, J.F., vani, C.V., Kumar, C.V., Bindhu, M.R., Sureshkumar, S., Al-Khattaf, F.S., Hatamleh, A.A., 2022. Efficient photocatalytic degradation of industrial contaminants by Piper longum mediated ZnO nanoparticles. *Environ. Res.* 208, 112686 <https://doi.org/10.1016/j.envres.2022.112686>.
- Asnicar, D., Fabrello, J., Ciscato, M., Masiero, L., Marin, M.G., Corami, F., Milan, M., Bernardini, I., Patarnello, T., Cecchetto, M., Giubilato, E., Bettoli, C., Semenzin, E., Matozzo, V., 2024. A multibiomarker approach in clams (*Ruditapes philippinarum*) for a toxicological evaluation of dredged sediments. *Environmental Pollution* 342, 123095. <https://doi.org/10.1016/j.enpol.2023.123095>.
- Bae, H.-D., Cho, M., Seo, H., Lyoo, I.K., Lee, K., 2023. Targeting the translationally controlled tumor protein by a monoclonal antibody improves allergic airway inflammation in mice. *Biomedicine & Pharmacotherapy* 168, 115655. <https://doi.org/10.1016/j.biopha.2023.115655>.
- Bordin, E.R., Ramsdorff, W.A., Lotti Domingos, L.M., de Souza Miranda, L.P., Mattoso Filho, N.P., Cestari, M.M., 2024. Ecotoxicological effects of zinc oxide nanoparticles (ZnO-NPs) on aquatic organisms: current research and emerging trends. *J. Environ. Manage.* 349, 119396. <https://doi.org/10.1016/j.jenvman.2023.119396>.
- Bouzidi, I., Khazri, A., Mougin, K., Bendhafer, W., Abu-Elsaoud, A.M., Plavan, O.-A., Ali, M.A.M., Plavan, G., Özdemir, S., Beyrem, H., Boufahja, F., Sélami, B., 2024. Doping zinc oxide and titanium dioxide nanoparticles with gold induces additional oxidative stress, membrane damage, and neurotoxicity in *Mytilus galloprovincialis*: results from a laboratory bioassay. *Journal of Trace Elements in Medicine and Biology* 83, 127401. <https://doi.org/10.1016/j.jtmb.2024.127401>.
- Çaykara, B., ÖzTÜRK, G., Alsaadoni, H., Ötünçtemur, A., Pençe, S., 2021. Evaluation of microRNA-124 expression in renal cell carcinoma. *Balkan Journal of Medical Genetics* 23, 73–78. <https://doi.org/10.2478/bjmg-2020-0029>.
- Cellura, C., Toubiana, M., Parrinello, N., Roch, P., 2006. HSP70 gene expression in *Mytilus galloprovincialis* hemocytes is triggered by moderate heat shock and *Vibrio anguillarum*, but not by *V. splendidus* or *Micrococcus lysodeikticus*. *Dev. Comp. Immunol.* 30, 984–997. <https://doi.org/10.1016/j.dci.2005.12.009>.
- Ciacci, C., Canonico, B., Bilanićová, D., Fabbri, R., Cortese, K., Gallo, G., Marcomini, A., Pojana, G., Canesi, L., 2012. Immunomodulation by Different Types of N-Oxides in the Hemocytes of the Marine Bivalve *Mytilus galloprovincialis*. *PLoS. One* 7, e36937. <https://doi.org/10.1371/journal.pone.0036937>.
- Destoumieux-Garzón, D., Canesi, L., Oyanedel, D., Travers, M., Charrière, G.M., Pruzzo, C., Vezzulli, L., 2020. *Vibrio* –bivalve interactions in health and disease. *Environ. Microbiol.* 22, 4323–4341. <https://doi.org/10.1111/1462-2920.15055>.
- Efthimiou, I., Kalamaras, G., Papavasileiou, K., Anastasi-Papathanasiou, N., Georgiou, Y., Dailianis, S., Deligiannakis, Y., Vlastos, D., 2021. ZnO, Ag and ZnO-Ag nanoparticles exhibit differential modes of toxic and oxidative action in hemocytes of mussel

- Mytilus galloprovincialis. *Science of The Total Environment* 767, 144699. <https://doi.org/10.1016/j.scitotenv.2020.144699>.
- Fatima, A., Zaheer, T., Pal, K., Abbas, R.Z., Akhtar, T., Ali, S., Mahmood, M.S., 2024. Zinc Oxide Nanoparticles Significant Role in Poultry and Novel Toxicological Mechanisms. *Biol. Trace Elem. Res.* 202, 268–290. <https://doi.org/10.1007/s12011-023-03651-x>.
- Franzellitti, S., Prada, F., Viarengo, A., Fabbri, E., 2020. Evaluating bivalve cytoprotective responses and their regulatory pathways in a climate change scenario. *Science of The Total Environment* 720, 137733. <https://doi.org/10.1016/j.scitotenv.2020.137733>.
- Kim, J., Kim, H.J., Choi, E., Cho, M., Choi, S., Jeon, M.A., Lee, J.S., Park, H., 2024. Expansion of the HSP70 gene family in *Tegillarca granosa* and expression profiles in response to zinc toxicity. *Cell Stress. Chaperones.* 29, 97–112. <https://doi.org/10.1016/j.cstres.2024.01.004>.
- Ku, J.H., Seo, S.Y., Kwak, C., Kim, H.H., 2012. The role of survivin and Bcl-2 in zinc-induced apoptosis in prostate cancer cells. *Urologic Oncology: Seminars and Original Investigations* 30, 562–568. <https://doi.org/10.1016/j.jurol.2010.06.001>.
- Lai, R.W.S., Zhou, G.-J., Yung, M.M.N., Djurišić, A.B., Leung, K.M.Y., 2023. Interactive effects of temperature and salinity on toxicity of zinc oxide nanoparticles towards the marine mussel *Xenostrobus securis*. *Science of The Total Environment* 889, 164254. <https://doi.org/10.1016/j.scitotenv.2023.164254>.
- Lima, I., Peck, M.R., Rendón-Von Osten, J., Soares, A.M.V.M., Guilhermino, L., Rotchell, J.M., 2008. Ras gene in marine mussels: a molecular level response to petrochemical exposure. *Mar. Pollut. Bull.* 56, 633–640. <https://doi.org/10.1016/j.marpolbul.2008.01.018>.
- Matei, E., Şăulean, A.A., Răpă, M., Constandache, A., Predescu, A.M., Coman, G., Berbecaru, A.C., Predescu, C., 2023. ZnO nanostructured matrix as nexus catalysts for the removal of emerging pollutants. *Environmental Science and Pollution Research* 30, 114779–114821. <https://doi.org/10.1007/s11356-023-30713-3>.
- Moreira, A.M.S., Freitas, E.T.F., Reis, M., de, P., Nogueira, J.M., Barbosa, N.P., de, U., Reis, A.I.M., Pelli, A., Camargo, P.R., da, S., Cardoso, A.V., de Paula, R.S., Jorge, E. C., 2023. Acute Exposure to Two Biocides Causes Morphological and Molecular Changes in the Gill Ciliary Epithelium of the Invasive Golden Mussel *Limnoperna fortunei* (Dunker, 1857). *Animals* 13, 3258. <https://doi.org/10.3390/ani13203258>.
- Ouagajou, Y., Aghzar, A., Presa, P., 2023. Population Genetic Divergence among Worldwide Gene Pools of the Mediterranean Mussel *Mytilus galloprovincialis*. *Animals* 13, 3754. <https://doi.org/10.3390/ani13243754>.
- Pei, T., Zhang, M., Nwanade, C.F., Meng, H., Bai, R., Wang, Z., Wang, R., Zhang, T., Liu, J., Yu, Z., 2024. Sequential expression of small heat shock proteins contributing to the cold response of *Haemaphysalis longicornis* (<scp>Acari: Ixodidae</scp>). *Pest. Manage. Sci.* <https://doi.org/10.1002/ps.7941>.
- Piccinno, F., Gottschalk, F., Seeger, S., Nowack, B., 2012. Industrial production quantities and uses of ten engineered nanomaterials in Europe and the world. *Journal of Nanoparticle Research* 14, 1109. <https://doi.org/10.1007/s11051-012-1109-9>.
- Pizzurro, F., Nerone, E., Ancora, M., Di Domenico, M., Mincarelli, L.F., Cammà, C., Salini, R., Di Renzo, L., Di Giacinto, F., Corbau, C., Bokan, I., Ferri, N., Recchi, S., 2023. Exposure of *Mytilus galloprovincialis* to Microplastics: accumulation, Depuration and Evaluation of the Expression Levels of a Selection of Molecular Biomarkers. *Animals* 14, 4. <https://doi.org/10.3390/ani14010004>.
- Romdhani, I., De Marco, G., Cappello, T., Ibala, S., Zitouni, N., Boughattas, I., Banni, M., 2022. Impact of environmental microplastics alone and mixed with benzo[a]pyrene on cellular and molecular responses of *Mytilus galloprovincialis*. *J. Hazard. Mater.* 435, 128952 <https://doi.org/10.1016/j.jhazmat.2022.128952>.
- Ruiz, P., Katsumiti, A., Nieto, J.A., Bori, J., Jimeno-Romero, A., Reip, P., Arostegui, I., Orbea, A., Cajaraville, M.P., 2015. Short-term effects on antioxidant enzymes and long-term genotoxic and carcinogenic potential of CuO nanoparticles compared to bulk CuO and ionic copper in mussels *Mytilus galloprovincialis*. *Mar. Environ. Res.* 111, 107–120. <https://doi.org/10.1016/j.marenvres.2015.07.018>.
- Sahibjam, F., Chambers, P., Kongara, K., Zhang, Y., Lopez, N., Jacob, A., Singh, P., Prabakar, S., 2024. Minimizing pain in deer antler removal: local anaesthetics in ZnO nanoparticle based collagen dressings as a promising solution. *European Journal of Pharmaceutics and Biopharmaceutics* 197, 114237. <https://doi.org/10.1016/j.ejpb.2024.114237>.
- Sturla Lompré, J., Giarratano, E., Gil, M.N., Malanga, G., 2024. Effect of acute cadmium exposure on oxidative stress and antioxidant system of the scallop *Aequipecten tehuelchus*. *Chemosphere* 352, 141512. <https://doi.org/10.1016/j.chemosphere.2024.141512>.
- Subramani, K., Inchraoensakdi, A., 2024. Physicochemical and photocatalytic properties of biogenic ZnO and its chitosan nanocomposites for UV-protection and antibacterial activity on coated textiles. *Int. J. Biol. Macromol.* 263, 130391 <https://doi.org/10.1016/j.ijbiomac.2024.130391>.
- Wang, W.-X., Meng, J., Weng, N., 2018. Trace metals in oysters: molecular and cellular mechanisms and ecotoxicological impacts. *Environ. Sci. Process. Impacts.* 20, 892–912. <https://doi.org/10.1039/C8EM00069G>.
- Weng, N., Meng, J., Huo, S., Wu, F., Wang, W.-X., 2022. Hemocytes of bivalve mollusks as cellular models in toxicological studies of metals and metal-based nanomaterials. *Environmental Pollution* 312, 120082. <https://doi.org/10.1016/j.envpol.2022.120082>.
- Wu, F., Cui, S., Sun, M., Xie, Z., Huang, W., Huang, X., Liu, L., Hu, M., Lu, W., Wang, Y., 2018. Combined effects of ZnO NPs and seawater acidification on the haemocyte parameters of thick shell mussel *Mytilus coruscus*. *Science of The Total Environment* 624, 820–830. <https://doi.org/10.1016/j.scitotenv.2017.12.168>.
- Wu, F., Sokolov, E.P., Khomich, A., Fettkenhauer, C., Schnell, G., Seitz, H., Sokolova, I. M., 2022. Interactive effects of ZnO nanoparticles and temperature on molecular and cellular stress responses of the blue mussel *Mytilus edulis*. *Science of The Total Environment* 818, 151785. <https://doi.org/10.1016/j.scitotenv.2021.151785>.
- Wu, F., Sokolova, I.M., 2021. Immune responses to ZnO nanoparticles are modulated by season and environmental temperature in the blue mussels *Mytilus edulis*. *Science of The Total Environment* 801, 149786. <https://doi.org/10.1016/j.scitotenv.2021.149786>.
- Xu, J., Xin-Ming, P.U., Lu, D., Xing, Y., Liu, C., Wei, M., Wang, B., Pan, J.-F., 2023. Seawater quality criteria and ecotoxicity risk assessment of zinc oxide nanoparticles based on data of resident marine organisms in China. *Science of The Total Environment* 905, 166690. <https://doi.org/10.1016/j.scitotenv.2023.166690>.
- You, L., Ning, X., Liu, F., Zhao, J., Wang, Q., Wu, H., 2013. The response profiles of HSPA12A and TCTP from *Mytilus galloprovincialis* to pathogen and cadmium challenge. *Fish. Shellfish. Immunol.* 35, 343–350. <https://doi.org/10.1016/j.fsi.2013.04.021>.
- Zhang, Y., Chen, S., Qin, X., Guo, A., Li, K., Chen, L., Yi, W., Deng, Z., Tay, F.R., Geng, W., Miao, L., Jiao, Y., Tao, B., 2024. A Versatile Chitosan-Based Hydrogel Accelerates Infected Wound Healing via Bacterial Elimination, Antioxidation, Immunoregulation, and Angiogenesis. *Adv. Healthc. Mater.* <https://doi.org/10.1002/adhm.202400318>.
- Zylicz, M., 2001. NEW EMBO MEMBERS' REVIEW: hsp70 interactions with the p53 tumour suppressor protein. *EMBO J.* 20, 4634–4638. <https://doi.org/10.1093/emboj/20.17.4634>.